Available online at www.sciencedirect.com
SCIENCE DIRECT®
International Journal of Heat and Fluid Flow 25 (2004) 320–328
International Journal of HEAT AND FLUID FLOW
www.elsevier.com/locate/ijhff

Evaporation of water drop on a plasma-irradiated hydrophilic surface

Y. Takata *, S. Hidaka, A. Yamashita, H. Yamamoto

Department of Mechanical Engineering Science, Faculty of Engineering, Kyushu University, 6-10-1 Hakozaki, Higashi-ku, Fukuoka 812-8581, Japan

Abstract

Experimental study has been performed on evaporation of water droplet on stainless steel, copper, and aluminum surfaces. These surfaces are exposed by the plasma irradiation to increase the wettability. We obtained the relation between the plasma irradiation and contact angle first, and then measured the evaporation time, the wetting limit temperature and the Leidenfrost temperature, increasing the surface temperature. The effect of plasma irradiation on evaporation curve has been examined. It is found that the evaporation time decreases and the wetting limit and the Leidenfrost temperatures increase as the contact angle decreases.

Keywords: Evaporation curve; Water drop; Contact angle; Wetting limit temperature; Wettability

1. Introduction

Solid surfaces irradiated by plasma become hydrophilic because the plasma particles remove the gas absorption layer and the active oxide layer appears on the surface. These rinse and activating effects reform the surface and increase its wettability for a certain period.

Fig. 1 explains how the surface is activated by plasma irradiation. Since the general metal surface has oxide layer of 30–40 Å and gas adsorption layer of 2–3 Å in thickness, its surface is not active compared with a fresh surface. In addition, the adhesion of dirt or oil materials makes the surface more hydrophobic. When such surface is irradiated by plasma, the dirt combines with plasma particles and is removed from the surface. Subsequently, oxide layer with high activity appears on the surface and this makes the surface hydrophilic. These rinse and activation effects drastically improve surface wettability for several hours.

The authors have studied the effect of wettability on various phase change heat transfer using photo-induced hydrophilicity of TiO_2 photocatalyst (Takata et al., 2000, 2001). It was found from the experiment of water drop evaporation that the lifetime of drop decreases and the wetting limit temperature (T_{WL}) increases as the contact angle decreases. Likewise, the plasma irradiation can be used to enhance the phase change heat transfer.

A number of studies on droplet evaporation can be found in the literature (Baumeister et al., 1966; Baumeister and Simon, 1973; Inada and Yang, 1993; McGinnis and Holman, 1969; Zhang and Yang, 1983). However the effect of surface wettability on evaporation characteristics has not yet been made clear up to now. One reason may be the difficulty in controlling the contact angle as only the exclusive parameter with the other parameters is unchanged. The plasma irradiation can be one of the solutions for this problem.

In the present study, we measured the contact angle of plasma-irradiated metallic surfaces to obtain the fundamental data for utilization of plasma irradiation. The relation between the contact angle and irradiation time for copper, aluminum and stainless steel was examined. The experiment of evaporation of single water drop was also performed to reveal the effect of wettability on the lifetime, the wetting limit temperature and the Leidenfrost temperature of water drop on hot surfaces. The experiment of immersion cooling of hot metal has also been performed to reveal that this technique can enhance the cooling rate in quenching process.

2. Experimental apparatus

Experimental apparatus is shown in Fig. 2. Single water droplet is injected to the hot surface ① from the

* Corresponding author. Tel.: +81-92-642-3398; fax: +81-92-642-3400.
E-mail address: takata@mech.kyushu-u.ac.jp (Y. Takata).

0142-727X/$ - see front matter © 2003 Elsevier Inc. All rights reserved.
doi:10.1016/j.ijheatfluidflow.2003.11.008

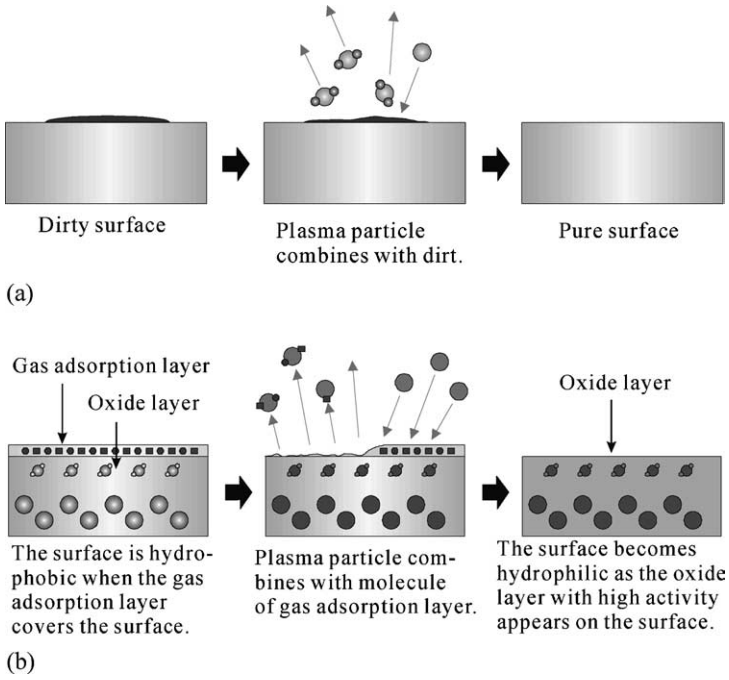

Fig. 1. Reaction of the surface by plasma irradiation: (a) effect of rinse and cleaning of grease, (b) effect of surface activation.

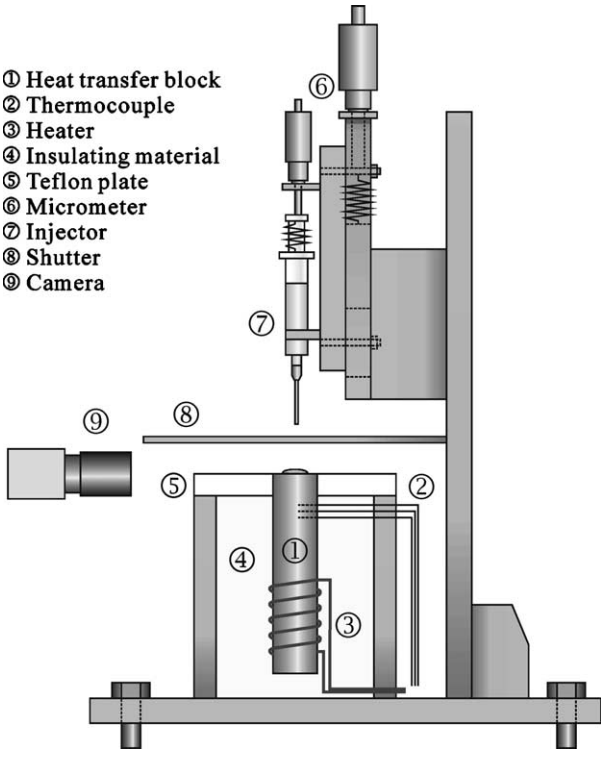

Fig. 2. Experimental apparatus.

syringe ⑦ and observed by digital high-speed camera and/or camcorder ⑨ during evaporation. The height of the needle is fixed to be 10 mm from the surface. The micrometer ⑥ is used to assure each droplet be constant size. Different sizes of needles are prepared to change the size of droplets. The droplet diameters are 2.16, 2.40, 2.66 and 2.96 mm and the corresponding Weber numbers are 5.18, 5.67, 6.19 and 6.72, respectively. Temperature of droplet is 20 °C in all experiments. The heat transfer surfaces used are cylinder of 30 mm in diameter in which three thermocouples are embedded at locations of 10, 15 and 20 mm from the top surface to measure the surface temperature. Three heat transfer surfaces illustrated in Fig. 3 are used; one is a flat surface and the others are two concave surfaces of 0.3 and 3 mm in depth at the center from outer rim.

When the surface temperature is low, the lifetime of droplet is measured with a timer. On the other hand, when the evaporation completes in short period, the lifetime is measured by counting the number of frames of the digital high-speed camera. The wetting limit temperature, T_{WL}, and the Leidenfrost temperature, T_{LEID}, were determined by the motion pictures of the digital high-speed camera or camcorder. Measurement of evaporation time was conducted by increasing the surface temperature with an increment of 10 K.

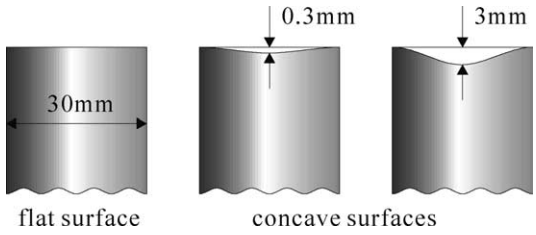

Fig. 3. Heat transfer copper surfaces.

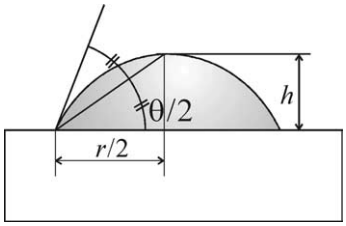

Fig. 4. Contact angle of water drop.

This apparatus is also used to measure contact angle. The measurements of contact angle have been done prior to each heat transfer experiment for flat surface. Single water droplet is injected to the surface from a syringe. To ensure the spherical shape, the size of water drop is less than 2 mm in diameter. The droplet on the surface is observed from the side by using camcorder and the magnified image of the droplet is displayed on monitor TV. By measuring its height and chord, as illustrated in Fig. 4, contact angle is given by

$$\theta = 2\tan^{-1}\left(\frac{2h}{r}\right) \quad (1)$$

on the assumption that the droplet on the surface forms a part of sphere. In each condition, the contact angles of five different locations are measured and averaged value is used as the contact angle.

Fig. 5(a) shows a plasma surface treater, ST-7000, produced by Keyence Corp., which generates arc plasma by discharging high voltage electricity (10 kV) from tungsten electrodes. The plasma particles are blown off toward the test surface by air stream of flow rate of 50 l/min as shown in Fig. 5(b). The frequency of plasma discharge ranges between 70 and 100 Hz in which the durations of discharge and intermission are 6–8 and 6 ms, respectively. The distance between the test surface and the plasma nozzle are 10 mm for copper and 7.5 mm for aluminum and stainless steel. These distances were selected by the recommendation by the user's manual of plasma generator, but there were not significant differences. The period of irradiation is usually 60–120 s in evaporation experiment.

3. Change in contact angle by plasma irradiation

Fig. 6 shows how contact angle decreases by the plasma irradiation for three different metals. Each metal surface was finished with mirror and emery papers of #600, #1000, #1500 and #2000. The initial contact angles are 89–102°, 53.6–81.8°, and 60.5–78.3° for copper, aluminum and stainless steel, respectively. The measurements of contact angles have been done immediately after the plasma irradiation at room temperature and relative humidity of about 60%. As seen from the figure, the contact angle decreases with the irradiation time. The contact angle decreases significantly in first five seconds and then gradually decreases afterwards. The data for copper scatters compared with other materials. The contact angles for these three materials decrease more rapidly as the surface becomes rough. The effect of surface roughness becomes smaller when the irradiation time passes over 100 s, and the terminal contact angles are 11°, 3° and 6° for copper, aluminum and stainless steel, respectively. The contact angle for surface finished by #600 emery paper decreases more rapidly than that of mirror finish. Among three metals, aluminum sample is the most hydrophilic.

Fig. 7 shows how contact angle increases after stopping irradiation. The metals and surface finish conditions are the same as indicated in Fig. 6. Durations of irradiation are 40, 60 and 120 s in each surface. As seen from the figure, surface becomes more hydrophilic as the duration of irradiation and the surface roughness increase.

The data for 120 s are connected by solid line. The data for copper scatters again significantly, while those for aluminum and stainless steel are well correlated. The tendencies for aluminum and stainless steel are similar to each other. The contact angle at 1 h of lapsed time

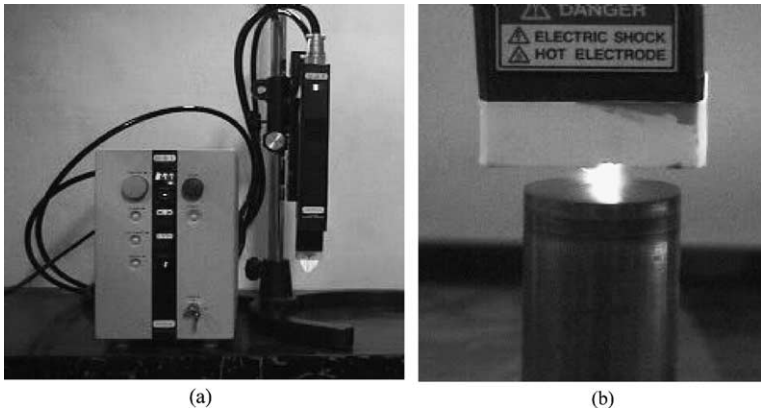

(a) (b)

Fig. 5. Plasma generator and irradiation to copper block: (a) plasma generator, (b) plasma irradiation.

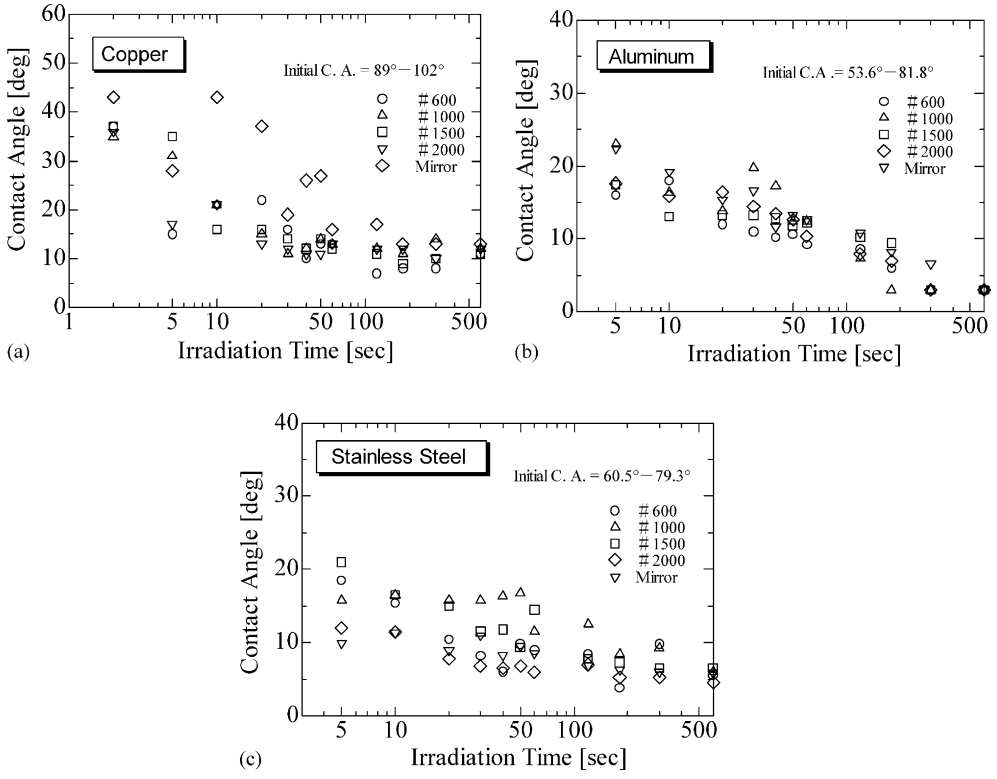

Fig. 6. Change in contact angle with irradiation time: (a) copper, (b) aluminum, (c) stainless steel.

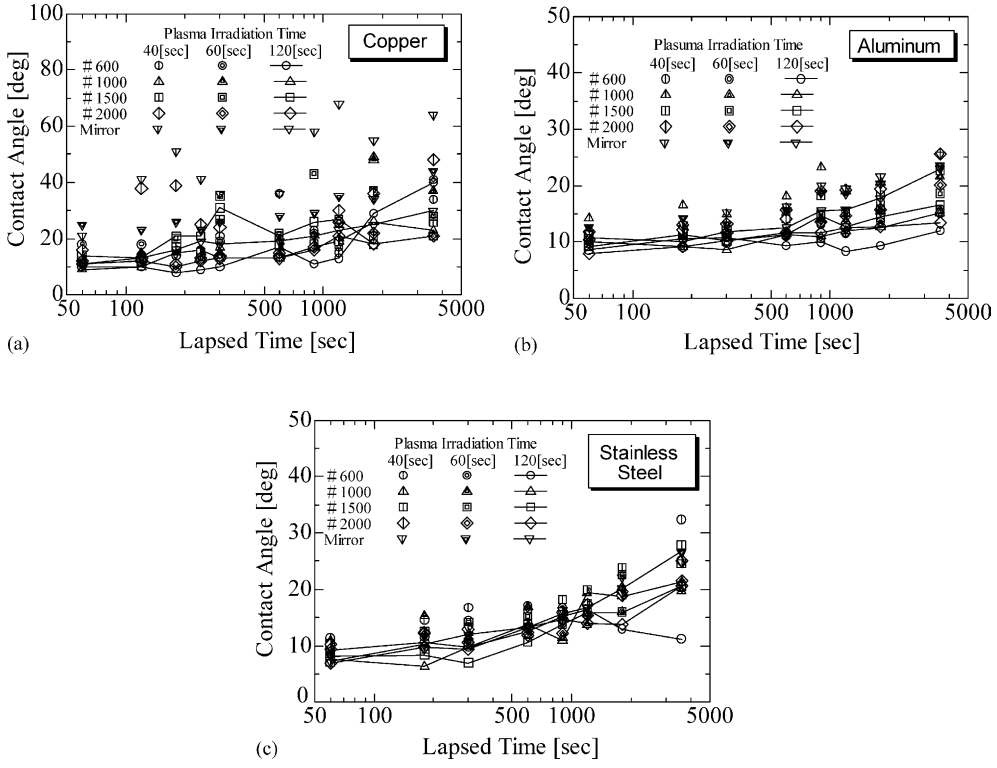

Fig. 7. Change in contact angle with lapsed time: (a) copper, (b) aluminum, (c) stainless steel.

ranges 19–64°, 12–26° and 11–32° for copper, aluminum and stainless steel, respectively. The best material is aluminum among three metals. Especially, the aluminum surface finished with #600 emery paper keeps the lowest contact angle. The reproducibility of change in contact angle was confirmed by the repeated measurements. All these repeated measurements showed the similar tendencies.

4. Experiments

4.1. Photographic observation of water drop behaviors

Experiment of water drop evaporation has been performed using three types of heat transfer surfaces as shown in Fig. 3. Copper, aluminum and stainless steel are used as the flat surfaces and whereas only the copper is used as concave surfaces. The range in surface temperature was from 50 to 180 °C. Each experimental run was recorded by either of the digital high-speed camera or the camcorder. The lifetime of water drop was obtained by analyzing the images of these cameras. The interval of each frame of the digital high-speed camera is 2 ms.

Typical photographs of water drop on both of normal and plasma-irradiated surfaces are shown in Fig. 8. The condition of the photographs is indicated in each caption. The contact angles for normal and plasma-irradiated surfaces are estimated as 73° and 10°, respectively. The irradiation time of plasma is 120 s and the irradiation is done just before each experimental run. The time indicated in caption is measured from the first collision of water drop to the surface.

Fig. 8(a) is for normal surface at $T_w = 130.2$ °C which is below the wetting limit and the Leidenfrost

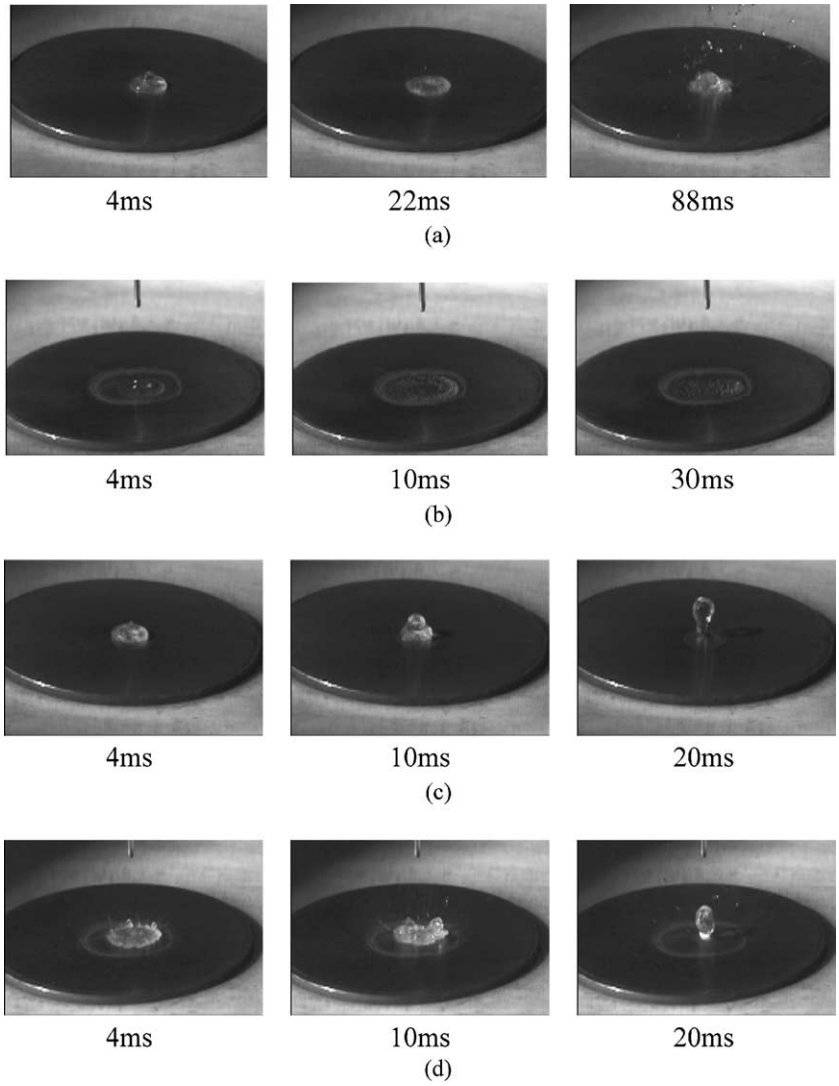

Fig. 8. Behavior of water drop on heated copper surface ($D = 2.66$ mm, concave surface with 0.3 mm in depth): (a) normal surface, $T_w = 130.2$ °C, (b) plasma-irradiated surface, $T_w = 130.0$ °C, (c) normal surface, $T_w = 170.6$ °C, (d) plasma-irradiated surface, $T_w = 169.9$ °C.

temperatures. At 4 ms, several tiny bubbles can be observed inside the droplet. Then the nucleation of bubbles occurs in whole droplet at 22 ms. The growth of these bubbles causes the scatter of tiny drops as shown in the right photograph (88 ms) of Fig. 8(a).

Fig. 8(b) is for plasma-irradiated surface at $T_w = 130.0$ °C and should be compared with Fig. 8(a). At 4 ms the droplet forms thin film on the surface because the surface wettability increases by the plasma irradiation. As observed in photograph at 10 ms, there are a number of tiny bubbles in the liquid film. The bubble population is dense in the outer rim of the film compared with the central zone. In the right photograph of Fig. 8(b), it is found that the size of liquid film at 20 ms becomes smaller than that at 10 ms because the intense evaporation at the outer rim of the film.

Fig. 8(c) and (d) show the droplet behavior at temperature higher than the Leidenfrost temperature. In the both photographs at 20 ms, droplet jumps upward from the surface and afterwards it becomes the Leidenfrost state. However, much difference between both cases can be observed in the left and the middle photographs. The droplet in Fig. 8(c) forms a hemisphere, whereas the droplet in Fig. 8(d) forms a film at 4 ms. In the initial stage of collision, the contact area between the droplet and the heating surface for plasma-irradiated surface is much larger than that for normal surface. Consequently, the lifetime of droplet on the plasma-irradiated surface becomes much shorter.

In low surface temperature, evaporation occurs at the film surface and the evaporation rate is rather small. Consequently the evaporation needs longer time. As the surface temperature increases, the evaporation becomes violently and the vapor film beneath the droplet is created immediately near T_{WL}. Such situation is schematically illustrated in Fig. 9. Violent evaporation forms the secondary droplet as shown in Fig. 9(c). It jumps upward and again falls onto the heated surface. If the surface temperature, T_W, is lower than T_{WL}, the secondary droplet contacts directly with the surface and repeats the similar sequence as shown in Fig. 9(b). On the other hand, when $T_W > T_{WL}$, the secondary droplet becomes Leidenfrost state as illustrated in Fig. 9(e). As the surface temperature becomes much higher than T_{WL}, the primary droplet itself jumps upward like Fig. 8(c) and (d). The determination of T_{WL} is done by analyzing images of the digital high-speed camera.

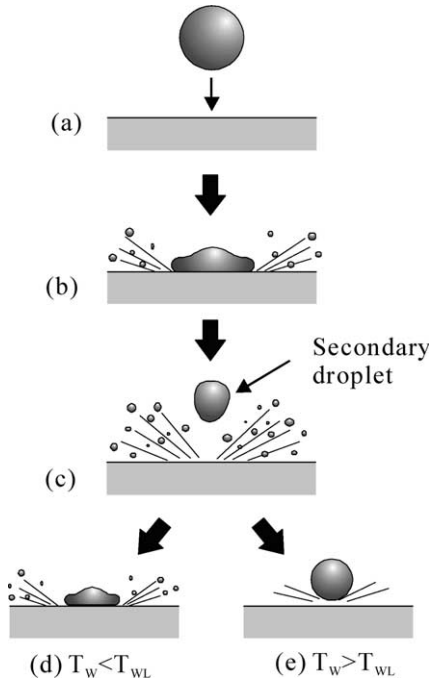

Fig. 9. Behavior of water drop near wetting limit temperature.

4.2. Evaporation curves for flat surfaces

Evaporation curves for flat surfaces of three metals are shown in Figs. 10–12. In each figure, (a) and (b) indicate the evaporation curves for normal and plasma-irradiated surfaces, respectively. Each surface was finished by #600 emery paper, and to keep low contact angle, the surface is irradiated by plasma for 120 s at an interval of 10 min. The sizes of droplet are 2.16, 2.40, 2.66 and 2.93, and the contact angles of each surface are

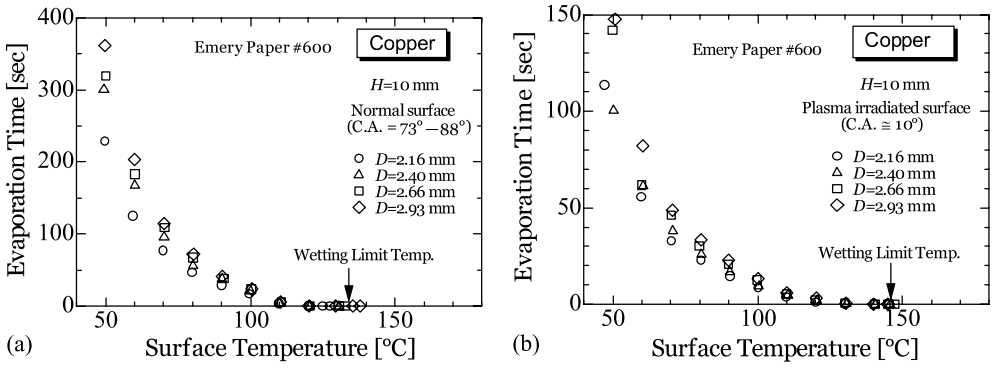

Fig. 10. Evaporation curve for flat copper surface: (a) normal surface, (b) plasma-irradiated surface.

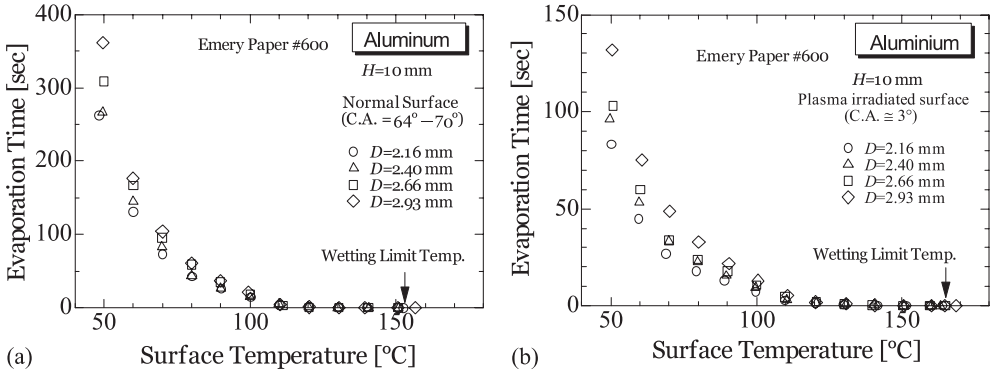

Fig. 11. Evaporation curve for flat aluminum surface: (a) normal surface, (b) plasma-irradiated surface.

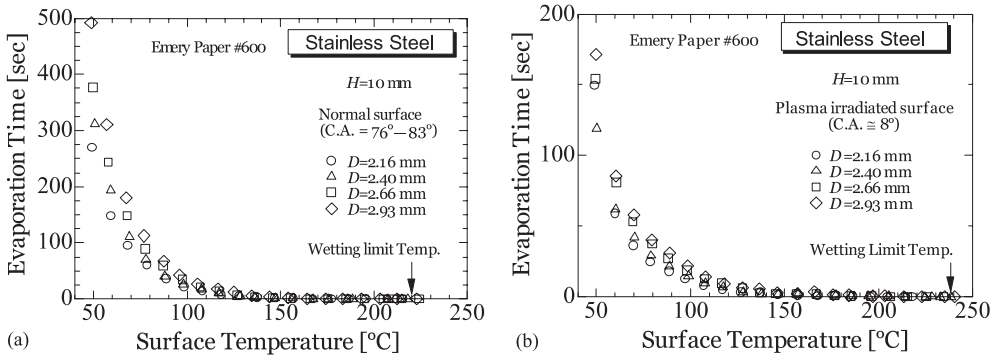

Fig. 12. Evaporation curve for flat stainless steel surface: (a) normal surface, (b) plasma-irradiated surface.

indicated in the figure. Since the droplet bounces out from the surface at higher surface temperature, the upper limit of measurement is T_{WL} for flat surfaces.

Fig. 10 shows evaporation curves for copper. It compares the result for normal surface (Fig. 10(a), $\theta = 73$–$88°$) and plasma-irradiated surface (Fig. 10(b), $\theta \approx 10°$). As seen from the figure, evaporation time for plasma-irradiated surface decreases significantly compared with that for normal surface especially in low surface temperature regions. This is obviously due to the improvement of surface wettability. In low surface temperature region, the evaporation time increases as the size of droplet increases, while the effect of droplet diameter is less significant in higher temperature region. It is also found that the evaporation time in Fig. 10(b) in lower temperature region dramatically decreases compared with Fig. 10(a). In addition, T_{WL} in Fig. 10(b) is by 15–18 K larger than that in Fig. 10(a). This is obviously due to the change in wettability of the surface. T_{WL} is almost independent of the size of droplet.

As seen in Figs. 11 and 12, the trends for aluminum and stainless steel are similar to Fig. 10. The value of T_{WL} for stainless steel is the largest among three metals because the thermal diffusivity is the lowest. The T_{WL}s for aluminum and stainless steel of plasma-irradiated surface are by 13 and 10–23 K higher than those for normal surface, respectively.

4.3. Evaporation curves for concave copper surfaces

The droplet on the flat surface bounces out from the surface above T_{WL} and hence the Leidenfrost temperature can hardly be measured. A concave heat transfer surface enables the measurement of the Leidenfrost temperature. Here, only the copper is used as the heat transfer surface.

Fig. 13(a) shows evaporation curves for a concave surface without plasma irradiation. The contact angle is 71–73° which is estimated from the data of the flat surface. The trend of evaporation curve is similar to the result of flat surface. The Leidenfrost temperature, T_{LEID}, is somewhat higher than the wetting limit temperature, T_{WL}. The detail near the Leidenfrost temperature is shown in Fig. 13(b). The data significantly scatter above T_{WL} and the dependence of droplet size on the evaporation time is not clear in this region.

Fig. 14(a) is the result for plasma-irradiated surface and Fig. 14(b) shows its magnification near the Leidenfrost temperature. The contact angle is estimated as 10°. As seen from both figures, evaporation time

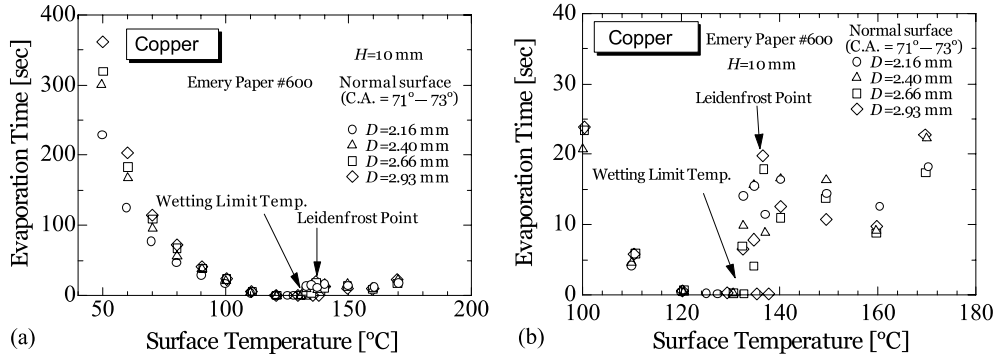

Fig. 13. Evaporation curve for normal copper concave surface: (a) whole temperature range, (b) near the Leidenfrost temperature.

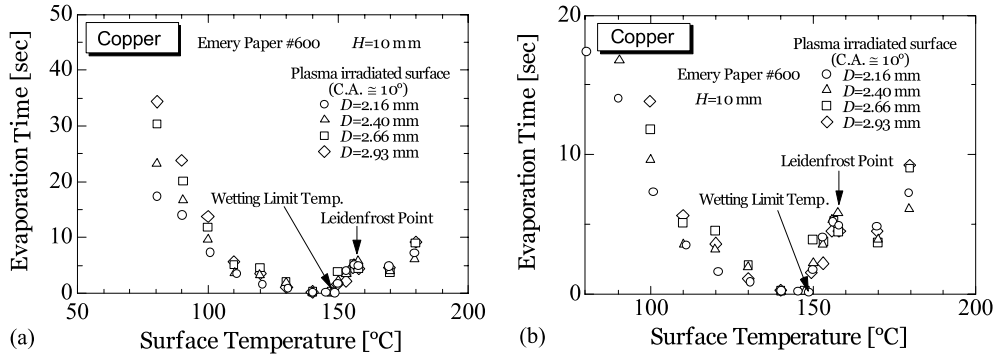

Fig. 14. Evaporation curve for plasma-irradiated copper concave surface: (a) whole temperature range, (b) near the Leidenfrost temperature.

decreases drastically compared with Fig. 13(a) and (b). For instance, the evaporation time at 80 °C for $D = 2.16$ mm of plasma-irradiated surface is one third of normal surface. In addition, values of T_{WL} and T_{LEID} for plasma-irradiated surface are by ~25 K higher than those for normal surface. The evaporation time in the region above T_{LEID} for plasma-irradiated surface also decreases compared with normal surface.

5. Concluding remarks

Experimental study has been performed on evaporation of water droplet on heated surface of stainless steel, copper, and aluminum. These surfaces are exposed by the plasma irradiation to increase the wettability. The relation between the plasma irradiation and contact angle was investigated first, and then the evaporation time and the wetting limit temperature of droplet were measured by increasing the surface temperature. The concave copper surface was also used to obtain the Leidenfrost temperature.

The results are summarized as follows:

1. Surfaces of copper, aluminum and stainless steel become hydrophilic by plasma irradiation. The terminal contact angle differs depending on the materials. The effect continues for a few hours after stopping irradiation.
2. The lifetime of water drop on the heated surface decreases significantly by plasma irradiation in the whole temperature range.
3. The wetting limit temperature, T_{WL}, and the Leidenfrost temperature, T_{LEID}, increase as the surface wettability increases.

Plasma-irradiation is an effective technique to increase surface wettability and can be used to enhance the phase change heat transfer.

Acknowledgements

This work was supported partly by the Kawasaki Steel 21st Century Foundation and the Grant-in-Aids for Scientific Research (B) 14350109 and on Priority Area 417 "Photo-Functional Interface" 14050072 from the Ministry of Science, Sports, Culture and Technology (MEXT).

References

Baumeister, K.J., Simon, F.F., 1973. Leidenfrost temperature—its correlation for liquid metals, cryogenics, hydrocarbons and water. Journal of Heat Transfer 95, 166–173.

Baumeister, K.J., Hamill, T.D., Schoessow, G.J., 1966. A generalized correlation of vaporization times of drops in film boiling on a flat plate. In: Proceedings of the 3rd International Heat Transfer Conference, vol. 3, pp. 66–73.

Inada, S., Yang, W.-J., 1993. Effects of heating surface materials on a liquid–solid contact state in a sessile drop-boiling system. Journal of Heat Transfer 115, 222–230.

McGinnis III, F.K., Holman, J.P., 1969. Individual droplet heat—transfer rates for splattering on hot surfaces. International Journal of Heat and Mass Transfer 12, 95–108.

Takata, Y., Hidaka, S., Cao, J.M., Masuda, M., Ito, T., Watanabe, T., Shimohigoshi, M., 2000. Boiling and evaporation from a superhydrophilic surface. Thermal Science and Engineering 8 (6), 33–41.

Takata, Y., Hidaka, S., Nakamura, T., Yamamoto, H., Masuda, M., Ito, T., 2001. Controlled contact angle and droplet evaporation using photo-induced hydrophilic surface. In: Proceedings of 2001 ASME International Mechanical Engineering Congress and Exposition, New York, NY (CD-ROM), IMECE 2001/HTD-24133.

Zhang, N., Yang, W.-J., 1983. Evaporation and explosion of liquid drops on a heated surface. Experiments in Fluids 1, 101–111.